Second-order cone programming relaxation-based multi-period reactive power optimization with VSC-Type HVDC and DFIG

Second-order cone programming relaxation-based multi-period reactive power optimization with VSC-Type HVDC and DFIG

Shixiong Fan [1], Wei Wang [1], Wei Han [1], Wei Wang [2], Peng Zhang [2], Xiaodong Shen[3, 4] and Yan Liu [3]

[1] China Electric Power Research Institute, Beijing, China;
[2] State Grid Gansu Electric Power Company;
[3] College of Electrical Engineering and Information Technology, Sichuan University.

[4] Email: shengxd@scu.edu.cn

Abstract. This paper presents a second order cone programming (SOCP) formulation of the dynamic reactive power optimization (DROPF) problem for the voltage source converter (VSC)-based high-voltage direct current (HVDC) transmission network, considering reactive power support of the doubly fed induction generator (DFIG). In this model, the reactive power support of DFIG, VAR compensators, the position of tap-changer and the states of VSC converters are formulated as continuous and discrete decision variables. By using approximation techniques, the original non-convex optimisation model is converted into a mixed-integer second-order cone programming model. Later, the SOCP formulation can be solved using many standard optimization packages. Then a DC system with VSC technology is modelled in the IEEE 30-bus example system. The SOCP formulation of AC-DC DROPF is applied to the modified IEEE 30-bus example system and the results are discussed.

1. Introduction

Compared with the AC system, the DC system has strong controllability, which provides a favorable control method for the power flow optimization of the hybrid AC/DC system. In [1], the reactive power optimization quadratic model of the AC/DC system is proposed and solved by the interior point method, but the discreteness of the control variables is not considered. Considering the regulating capacity of DC power transmission system to power and voltage, a new model of dynamic reactive power optimization of AC/DC system is proposed in [2].The objective of the model is to minimize all-day network loss of the AC/DC system. In [3], a new strategy is proposed to optimizing reactive power of AC/DC power system, based on singular value decomposition and predictor-corrector primal-dual interior point algorithm. In [4], In order to minimize both active power loss and square sum of voltage deviation in all key nodes, a multi-objective reactive power optimization model of AC/DC interconnection system was built and an improved normalized normal constraint method was proposed to obtain Pareto optimal solutions of this model. In order to avoid frequent power regulation of DC transmission lines, a dynamic reactive power optimization model of AC/DC power systems, which takes into consideration the DC power regulation limits, is established and then solved by using the generalized Benders decomposition[5].

Conventionally two types of converter, voltage source converters (VSCs) and current source converters (CSCs), are employed for two terminal HVDC links. Especially, the voltage source

converters (VSCs) are suitable for HVDC systems, compared to the current source converters (CSCs), since VSCs can regulate the reactive and active power in such a way to maintain the AC side voltage. VSCs offer more flexibility than what CSCs do[6], where only the active power can be modulated. [7] presents a second order cone programming (SOCP) formulation of the optimal power flow problem for AC-DC systems with voltage source converter (VSC) technology. Approximation techniques have been used to derive the SOCP formulation of the AC-DC OPF problem. [8] develops an OPF with the hybrid VSC-HVDC transmission and active distribution networks to optimally schedule the generation output and voltage regulation of both networks, which leads to a non-convex programming model. Furthermore, the non-convex power flow equations are based on the second-order cone programming (SOCP) relaxation approach. SOCP relaxation approach is used since there are great advantages to recognizing a convex optimization problem. One advantage is that the problem can be solved very reliably and efficiently. Another is related to theoretical or conceptual advantages of formulating a problem as a convex optimization problem, such that the global optimal solution can be guaranteed by Karush–Kuhn–Tucker conditions. [9] presents an optimal reactive power flow model with voltage source converters, which is solved by branch and bound method and primal dual interior point method.

A dynamic reactive power optimization model with VSC and considering reactive power support of the DFIG is proposed. The reactive power support of DFIG, VAR compensators, the position of tap-changer and the states of VSC converters are formulated as continuous and discrete decision variables. By using approximation techniques, the original non-convex optimization model is converted into a mixed-integer second-order cone programming model.

The remaining of this paper is organized as follows: Section 2 presents a general ROPF model considering the VSC-HVDC and reactive power support of DFIG-based wind turbines. In Section 3, the SOCP relaxation method is proposed to efficiently solve the proposed model. Furthermore, numerical results on test systems demonstrate the effectiveness of the proposed method in Section 4. Finally, conclusions are drawn in Section 5.

2. Multi-period reactive power optimization considering VSC and DFIG

In this paper, considering VSC and DFIG, operation of tap-changer is investigated to minimize energy loss over multiple periods while maintaining the voltage magnitude within a desirable range. The specific optimization models with physical constraints are formulated as follows:

2.1. Objective function

The objective of the model is the minimum all-day network loss of the AC/DC grid. This is described as:

$$\min \quad \sum_{t=1}^{T} P_t^{loss} = \sum_{t=1}^{T} \sum_{ij \in E} \left(r_{ij} I_{ij,t}^2 \right) \tag{1}$$

Where, T is the number of periods; E is the set of branches; r_{ij} is the resistance of branch (i, j); $I_{ij,t}$ is the current of branch (i, j) at time period *t*.

2.2. AC line flow constraints

Let consider a conventional direction for each line starting from sending bus and ending to receiving bus. The active and reactive power balance equations for AC node other than PCCs can be written as follows:

$$P_{j,t} = \sum_{k \in \delta(j)} P_{jk,t} - \sum_{i \in \pi(j)} \left(P_{ij,t} - r_{ij} \%\!\!\%_{ij,t} \right) + g_j \%\!\!\%_{j,t}, \forall t, \forall j \in AC\_B \tag{2a}$$

$$Q_{j,t} = \sum_{k \in \delta(j)} Q_{jk,t} - \sum_{i \in \pi(j)} \left(Q_{ij,t} - x_{ij} \%\!\!\%_{ij,t} \right) + b_j \%\!\!\%_{j,t}, \forall t, \forall j \in AC\_B \tag{2b}$$

$$\%\!\!\%_{j,t} = \%\!\!\%_{i,t} - 2\left(P_{ij,t} r_{ij} + Q_{ij,t} x_{ij} \right) + \%\!\!\%_{ij,t} \left(r_{ij}^2 + x_{ij}^2 \right), \forall ij \in AC\_E \tag{2c}$$

$$\%I_{ij,t} = \frac{P_{ij,t}^2 + Q_{ij,t}^2}{\%V_{i,t}}, \forall t, \forall ij \in AC\_E \tag{2d}$$

$$P_{j,t} = P_{j,t}^g + P_{j,t}^W - P_{j,t}^L \tag{2e}$$

$$Q_{j,t} = Q_{j,t}^g + Q_{j,t}^{\mathrm{W}} + Q_{j,t}^C + Q_{j,t}^{CB} - Q_{j,t}^L \tag{2f}$$

Where

$$\%V_{i,t} = V_{i,t}^2 \ , \ \%I_{ij,t} = I_{ij,t}^2$$

AC_B and AC_E are nodes and branch sets in the AC system, respectively; $\delta(j)$ is the set of all parents of bus j, $\pi(j)$ is the set of all children of bus j; x_{ij} is the reactance of branch (i, j); g_j / b_j is the shunt conductance/susceptance from bus j to ground; $V_{i,t}$ voltage of bus j at time period t. $P_{j,t}$ and $Q_{j,t}$ are active and reactive power at bus j at time period t, respectively. $P_{j,t}^g / Q^g{}_{j,t}$, $P_{j,t}^W / Q_{j,t}^{\mathrm{W}}$, $P_{j,t}^L / Q_{j,t}^L$ are active/reactive power flow of dispatched thermal generation, DFIG and load at bus j at time period t, respectively. $Q_{j,t}^C$ and $Q_{j,t}^{CB}$ are reactive of the static var compensators and the capacitor banks, respectively.

2.3. VSC converter constraints

In this paper, the impedance of the converter station $R_{VSC,i} + jX_{VSC,i}$ is equivalent to the AC branch, which is combined into the AC system for processing, so the active power of the input VSC is equal to the DC power of the VSC output, namely:

$$P_{VSC,i,t} = P_{dc,i,t}, \quad \forall t, \forall i \in VSC\_B \tag{3a}$$

Where, VSC_B is the set of the point of common connection (PCC).

In addition, $V_{VSC,i,t} \angle \theta_{VSC,i,t}$ satisfy the following relationship [10]:

$$V_{VSC,i,t} = \frac{\sqrt{3}}{2} \mu M_{i,t} V_{dc,i,t}, \forall t, \forall i \in VSC\_B \tag{3b}$$

Where, μ is power transfer efficiency of converter, and $0 \le \mu \le 1$; When the modulation model is SPWM, $\mu = \frac{\sqrt{3}}{2}$; When the modulation model is SVPWM, $\mu = 1$; M is the modulation factor of VSCs. In this paper, we set $\mu = \frac{\sqrt{3}}{2}$ and $0 \le M \le 1$.

2.4. OLTC constraints

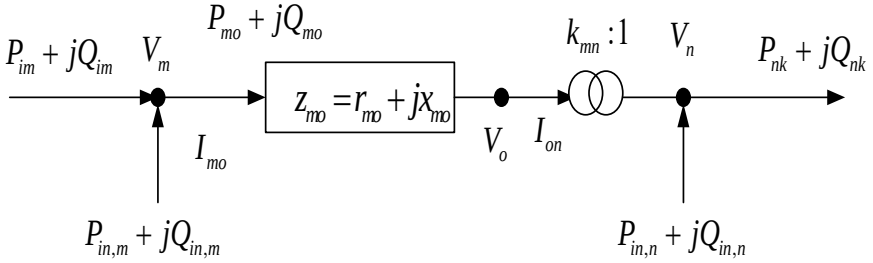

Figure 1. Branch flow model with OLTC.

The model of the OLTC model is shown in Figure 1, and the virtual node o is introduced. The equivalent impedance of the branch (*m*,*o*) is $z_{mo} = r_{mo} + jx_{mo}$,which can be regarded as a conventional AC branch processing . The voltage of the virtual node o is

$$\overset{\%}{V}_{o,t} = k_{mn}^2 \overset{\%}{V}_{n,t}, \quad \forall t, \forall o \in B^{oltc} \tag{4a}$$

Where, B^{oltc} is the set of virtual nodes with OLTC; k_{mn} is the tap ratio of OLTC branch (*m*,*n*), which is the discrete variables; $\overset{\%}{V}_{o,t}$ and $\overset{\%}{V}_{n,t}$ are square of voltage magnitude of node *o* and *n*, respectively; Set $K_{o,t} = k_{mn}^2$, then

$$\overset{\%}{V}_{o,t} = K_{o,t} \overset{\%}{V}_{n,t}, \quad \forall t, \forall o \in B^{oltc} \tag{4b}$$

Since $K_{o,t}$ is a non-integer discrete variable, the following transformation needs to be conducted in calculations:

$$K_{o,t} = \underline{K}_o + \sum_m \Delta K_{o,m} \sigma_{o,t,m}^{OLTC}, \forall t, \forall o \in B^{oltc} \tag{4c}$$

Where, $\underline{K}_o$ is the lower bound of square of tap ratio for OLTC connected to bus *j*; $\Delta K_{o,m}$ is step size of square of tap ratio; $\sigma_{o,t,m}^{OLTC}$ is a dummy binary variable for bus j equipped with OLTC.

Moreover, in practical operations the tap change times for an OLTC are strictly constrained, that is,

$$\sigma_{o,t,SR_o}^{OLTC} \le \sigma_{o,t,2}^{OLTC} \le \sigma_{o,t,1}^{OLTC} \tag{4d}$$

$$\delta_{o,t}^{OLTC,IN} + \delta_{o,t}^{OLTC,DE} \le 1 \tag{4e}$$

$$\sum_m \sigma_{o,t,m}^{OLTC} - \sum_m \sigma_{o,t-1,m}^{OLTC} \ge \delta_{o,t}^{OLTC,IN} - \delta_{o,t}^{OLTC,DE} SR_o \tag{4f}$$

$$\sum_m \sigma_{o,t,m}^{OLTC} - \sum_m \sigma_{o,t-1,m}^{OLTC} \le \delta_{o,t}^{OLTC,IN} SR_o - \delta_{o,t}^{OLTC,DE} \tag{4g}$$

$$\sum_{t \in T} \left(\delta_{o,t}^{OLTC,IN} + \delta_{o,t}^{OLTC,DE} \right) \le \overline{N}_o^{OLTC}, \forall t, \forall o \in B^{oltc} \tag{4h}$$

Where, $\delta_{o,t}^{OLTC,IN}$ and $\delta_{o,t}^{OLTC,DE}$ are regulation status of OLTC bus o at time t, which indicate that the tap positions cannot increase and decrease simultaneously. SR_o is the range of regulation of OLTC connected to bus *o*. $\overline{N}_o^{OLTC}$ is the maximum of regulation number of OLTC connected to bus *o*.

2.5. DFIG-based wind power constraints

In most practical cases of China, the typically centralized integrated wind farms are widely used. In the traditional optimization model, due to the constant power factor control mode is generally adopted, the wind farms reactive power output is regarded as a fixed value, which cannot fully reflect the reactive power output characteristics of the wind farms. This paper uses the capacity curve of the wind farms to analyze its reactive support capacity. The linearized method can be used to obtain the model of the DFIG [11], which are:

$$P_{j,t}^W \le \frac{P_{j,t}^{W1}}{Q_j^{W1} - \underline{Q}_j^W} \left(Q_{j,t}^W - \underline{Q}_j^W \right) \tag{5a}$$

$$P_{j,t}^W \le \frac{P_j^{W2} - P_j^{W1}}{Q_j^{W2} - \underline{Q}_j^{W1}} \left(Q_{j,t}^W - Q_j^{W1} \right) + P_j^{W1} \tag{5b}$$

$$P_{j,t}^{W} \le \frac{P_j^{W3} - P_j^{W2}}{Q_j^{W3} - \underline{Q}_j^{W2}} \left(Q_{j,t}^{W} - Q_j^{W2} \right) + P_j^{W2} \quad (5c) \qquad P_{j,t}^{W} \le \frac{P_j^{W4} - P_j^{W3}}{Q_j^{W4} - \underline{Q}_j^{W3}} \left(Q_{j,t}^{W} - Q_j^{W3} \right) + P_j^{W3} \quad (5d)$$

$$P_{j,t}^{W} \le \frac{P_j^{W4}}{Q_j^{W4} - \overline{Q}_j^{W3}} \left(Q_{j,t}^{W} - \overline{Q}_j^{W} \right) \quad (5e)$$

Where, $P_{j,t}^{W}$ are $Q_{j,t}^{W}$ the active and reactive power of the DFIG-based wind at time *t*, respectively; ($\underline{Q}_j^{W}$,0), (Q_j^{W1},P_j^{W1}), (Q_j^{W2},P_j^{W2}), (Q_j^{W3},P_j^{W3}), (Q_j^{W4},P_j^{W4}) and ($\overline{Q}_j^{W}$,0) are the 6 corresponding feature points of the DFIG-based wind.

2.6. Security Constraints

The security constraints include:

- AC/DC control variables including real and reactive power generations, controlled shunt capacitors, tap-changing;
- AC/DC network security constraints including AC/DC transmission flow and bus voltage limits, and limits to DC currents, voltages, and power of converters;

3. Proposed SOCP relaxation

Obviously, the DROPF model of (1)-(4) is a non-convex programming model due to the non-convexity resulted from the non-convex power flow equations, whose global optimal solutions are difficult to obtain. Generally, it is expected that the relaxed model is a convex problem, since there are great advantages to recognizing a convex optimization problem.

Now, (2d) can be reformulated as standard second-order conic constraints as:

$$\left\| \begin{matrix} 2P_{ij,t} \\ 2Q_{ij,t} \\ \tilde{I}_{ij,t} - \tilde{V}_{j,t} \end{matrix} \right\|_2 \le \tilde{I}_{ij,t} + \tilde{V}_{j,t}, \quad \forall ij \in AC\_E \quad (6a)$$

However, the constraint (3b) is non-convex quadratic equalities. Then, the conic relaxation is performed by relaxing the quadratic equalities into inequalities. Thus, it yields [10]:

$$V_{VSC,i,t} \le 0.5 V_{dc,i,t}, \forall t, \forall i \in VSC\_B \quad (6b)$$

After relaxation, the formula is a SOCP model with mixed integer variables. There are many standard optimization packages (e.g. CPLEX, MOSEK, GUROBI etc.) that can be used to efficiently solve the SOCP.

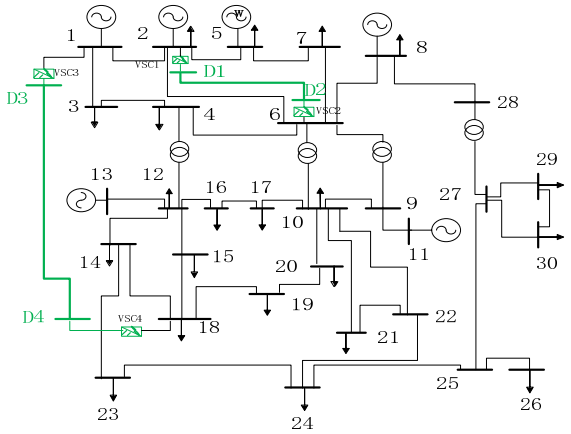

Figure 2. Modified IEEE 30-bus test system with embedded DC system.

Table 1. Branch parameters in DC network.

T_{BUS}	F_{BUS}	r/p.u.
2	6	0.037
1	18	0.047

4. Numerical examples

4.1. Modified IEEE 30-bus test system with embedded DC system

To evaluate the proposed model, the IEEE 30-bus test system is modified and as shown in Figure 2. The detailed original parameters of IEEE 30-bus test system are obtained from MATPOWER. Converters VSC1, VSC2, VSC3 and VSC4 are connected to AC buses 2, 6, 1and 18, respectively. Since DC grid and their associated converters have not been implemented in MATPOWER software, we give the detailed parameters of DC branch in Table 1.

4.2. Optimization result analysis

The total power loss rate before the optimization is 5.26%, while the loss rate optimized is 3.41%, reducing the loss rate of 1.85%. It is worth noting that the optimized loss is the result of power flow calculation based on the AC/DC power flow equation after the fixed capacitor switching state and the unit reactive power output, thus ensuring the accuracy of the network loss calculation result.

Figure 3 and Figure 4 show the optimal distribution strategy for optimal power and DC node voltage for AC-DC parallel lines throughout the day. It can be seen from the figure that the total active power transmitted by the AC and DC sections in different time periods is different, and the power allocated by the DC parallel lines is also different. Therefore, when the active power of the AC-DC section transmission changes, in order to achieve the minimum network loss, the transmission power of the DC line should be adjusted, and the constant power control mode cannot be used to maintain the DC power. Relative AC system reactive power compensation and transformers, HVDC transmission power in order to meet changing requirements, require frequent adjustment coordinated control apparatus converter stations, in order to make the system run at the optimal state. Therefore, the literature [7] suggests not setting the control mode of the VSC before optimization, but using it as an optimization variable to set the control mode according to the optimized result.

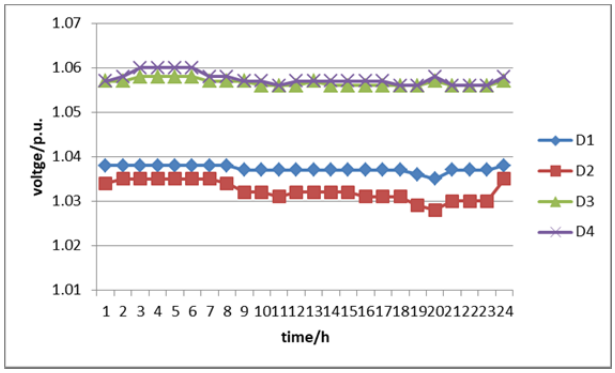

Figure 3. Curve of voltage of the DC node.

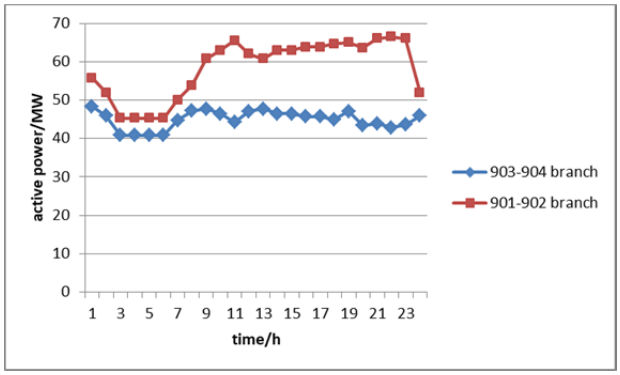

Figure 4. Curve of power flow of the DC branch.

Influence of reactive power support capacity of DFIG

In the traditional power grid optimization, it doesn't consider the reactive power support capability of the DFIG, but merely considers the simple constraints of its active and reactive upper and lower limits. In this paper, the capacity curve is used to characterize the DFIG active and reactive coupling with reactive power support. Considering of the reactive power of the DFIG, the system loss will be smaller than the case of neglecting its reactive power, That is, the system will get better optimization effect than before considering the reactive power support capability of the DFIG. At the same time, Figure 5 shows that when considering the reactive power output of the DFIG, the required reactive power compensation device will decrease, especially during the peak load period, because DFIG provides powerful reactive power support.

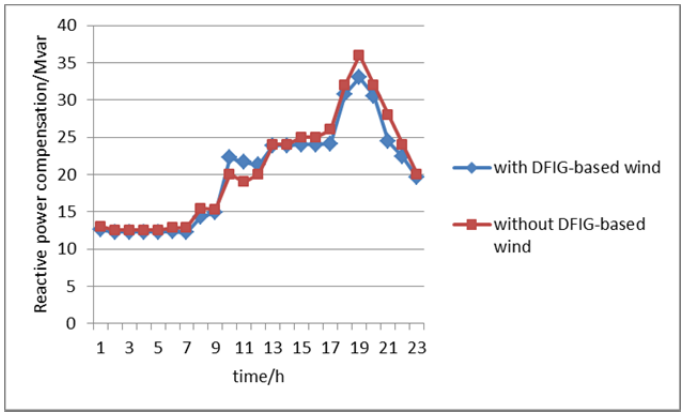

Figure 5. Comparison for the reactive power compensation with/without DFIG.

5. Conclusions

In this paper, the dynamic reactive power optimization model considering VSC and DFIG is established. Through the analysis of the example, the following conclusions are obtained:

1) The reactive power regulation of the converter station is bidirectional, which is significantly different from the capacitor reactive compensation in the conventional AC grid;

2) Considering the DFIG reactive power support capability, the system loss will be smaller than the case of ignoring its reactive power, and will get better optimization results than before. When considering DFIG reactive power, the required reactive power compensation device will decrease, especially during the peak load period, because DFIG provides powerful reactive power support.

Acknowledgments

Project Supported by Science and Technology Foundation of State Grid Corporation of China (DZ71-17-011)

References

[1] Yu J, Yan W, Li W, et al. 2008 *Electric Power Systems Research* **78(3)** 302-310
[2] YAN Wei, ZHANG Haibing, TIAN Tian, et al. 2009 *Automation of Electric Power Systems* **33(10)** 43-46
[3] Ding Tao, Li Huaqiang, Fan Pei 2009 *Transactions of China Electrotechnical Society* **24(2)** 158-163
[4] LI Qing, LIU Mingbo, YANG Liuqing 2014 *Proceedings of the CSEE* **34(7)** 1150-1158
[5] LI Qing, LIU Ming-bo, ZHAO Wen-meng 2016 *Journal of South China University of Technology (Natural Science Edition)* **44(4)** 55-62
[6] Liu H, Chen Z 2015 *IEEE Transactions on Energy Conversion* **30(3)** 918-926
[7] Baradar M, Hesamzadeh M R, Ghandhari M 2013 *IEEE Transactions on Power Systems* **28(4)** 4282-4291
[8] Ding T, Li C, Yang Y, et al. 2017 *IET Generation Transmission & Distribution* **11(15)** 3665-3674
[9] YU Xiuyue, SONG Shaoqun, GUO Ruipeng, et al. 2017 *Power System Protection and Control* **45(19)** 148-153
[10] WANG Shouxiang, CHEN Sijia, XIE Songguo 2017 *Automation of Electric Power Systems* **41(11)** 85-91
[11] Rueda-Medina A C, Franco J F, Rider M J, et al. 2013 *Electric Power Systems Research* **97(1)** 133-143